Analysis of Grouser Performance to Develop Guidelines for Design for Planetary Rovers

Hiroaki Inotsume*, Krzysztof Skonieczny*[1]*, David S. Wettergreen*

*Field Robotics Center, Carnegie Mellon University, Pittsburgh, PA 15213, USA
e-mail: {hinotsume,dsw}@cmu.edu
kskoniec@alumni.cmu.edu

Abstract

This paper addresses issues in the design of wheel grousers for planetary rovers. It has been shown in prior and related work that grousers on wheel rims can improve traveling performance of rovers on loose soils. However, the main focus of these studies, so far, has been limited to straight grousers and to straight line motion of the wheels. This work extends such studies to include chevron-shaped grousers and also sideslipping motions for cross-slope and steering maneuvers. We show that chevron-shaped grousers can increase tractive efficiency (the ratio of output to input work for the wheel), though only in relatively benign or low slip operations. We also show that grousers increase lateral forces during sideslip operations, improving performance on cross-slopes, but decreasing skid-steering efficiency. We demonstrate that an equation for appropriate grouser spacing, developed in prior work, remains consistent with sideslip operations. Based on these results, guidelines for grouser design are discussed for different operating conditions.

1 Introduction

When planetary rovers traverse on terrain covered with loose, granular regolith, wheels can lose their traction resulting in high slip and sinkage. After the entrapment of NASA's Mars Exploration Rovers in Martian regolith, the importance of wheel slip and sinkage and of understanding wheel-soil interactions came to be widely recognized.

Considerable research has been, thus far, conducted to study wheel designs to improve vehicles' traversing performance on granular materials, and it has been acknowledged that a wheels tread pattern, or grousers, can have an important role for obtaining better traction on loose soils. Bauer et al., for example, reported that the increase of the number of grousers makes improvement of traction [1]. Sutoh et al. also studied the influence of the number of grousers and found that the improvement by the increase of grouser number has a limitation when the spacing between grousers become small [2]. Ding et al. studied the grouser performance on loose soil with various grouser configurations, and reported that the height of grousers also largely influences the performance of wheels in addition to the number of grousers [3]. In addition to the experimental-based evaluations of grouser performance, researchers has been tying to model the grouser-soil interactions. Irani et al. developed a Terramechanics-based wheel-soil interaction model incorporating the dynamic behavior of grousered wheels [4]. They assumes that the grousers bulldoze the soil and gain reactive force from the soil, and compared simulation results with results of experiments. Nakashima et al., on the other hand, developed an analytical model of a wheel with grousers using a discrete element method, and conducted numerical simulations as well as experimentation for slope ascent [5].

Although several grouser studies have been conducted, there exist few guidelines for designing grousers for planetary rover applications. In one such study, Skonieczny [6] suggested a guideline for grouser spacing from another perspective. They analyzed the soil flow induced by grousers and found wheels with an appropriate number of grousers can reduce the resistive forward soil flow in front of the wheel. From this observation, they proposed an equation for the grouser spacing to reduce the forward soil flow and increase the wheel performance.

Most research on grousers, including the abovementioned guidelines of grouser design, have been limited to straight line motions of wheel/rovers. However, actual rover operations also involve lateral motions, including steering maneuver and traverse of cross slopes, causing sideslip. Also, most of the grouser studies for planetary rovers have been restricted only to simple, straight-shaped grousers while there are more parameters to be considered, such as orientation and inclination angle of grousers.

The purpose of this study is to further develop comprehensive guidelines for design of wheels with grousers. To this end, we studied the lateral traversing performance of grousered wheels as well as the longitudinal performances based on single wheel experiments. In addition to the straight grousers, chevon-shaped grousers were also assessed. The remainder of this paper is as follows. Sec-

*[1]Dr. Skonieczny is now at Electrical and Computer Engineering, Concordia University, Montreal, QC H3G 2W1, Canada

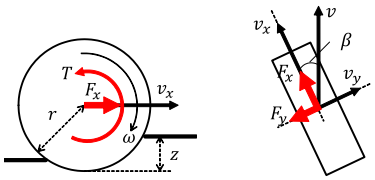

(a) straight traveling (b) steering

Figure 1. Straight travel and steering maneuver.

tion 2 defines the evaluation criteria of traversing performance of wheels. Section 3 reviews the grouser spacing equation developed in [6], and shows experimental validation for different heights of grousers and different soil materials. In Section 4, the influence of the grouser spacing and height on wheel steering performance are evaluated based on experiments. In section 5, the influence of the chevron angles of grousers are assessed in terms of both the straight travel and steering performances. Guidelines to design grousers will be discussed in Section 6 depending on steering methods of rovers and target terrain for operations, and Section 7 concludes the paper.

2 Evaluation Criteria

Planetary rovers operate in various conditions including simple straight line traverse, steering motions on level ground (Figure 1), as well as traverse of inclined terrain (Figure 2).

One criterion to evaluate the performance of a wheel is its relationship between slip and the tractive force it can gain from the soil. In the case of straight travel on level terrain shown in Figure 1 (a), a wheel can slip in the longitudinal direction, and the longitudinal slip can be measured as slip ratio s defined as the ratio of the actual travel velocity v_x to the wheel tangential velocity $r\omega$ [7]:

$$s = 1 - \frac{v_x}{r\omega} \tag{1}$$

where r is the radius of the wheel, and the ω is the wheel angular velocity. In this study, the length from the center of the wheel to the tip of a grouser is used as the radius r. A net tractive longitudinal force is defined as drawbar pull F_x. Sinkage z is another important criterion to assess wheel performance. One more criterion is tractive efficiency η which indicates how efficiently the wheel can travel on the target soil and is defined as the ratio between the output and input work of the wheel as follows:

$$\eta = \frac{F_x \cdot r(1-s)}{T} \tag{2}$$

where T is the resistance torque required for the wheel rotation. In this paper, the relation between the slip ratio and the drawbar pull, sinkage and/or tractive efficiency will

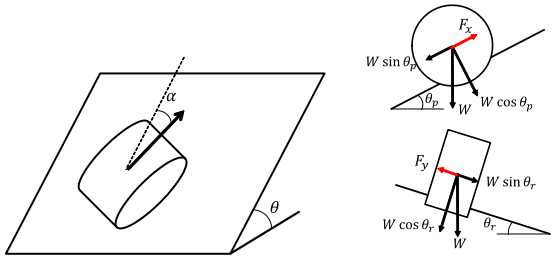

Figure 2. Slope ascent with an attack angle.

be used to assess straight travel performance of grousered wheels.

On the other hand, slip in the lateral direction is also generated in addition to the longitudinal slip when the wheel/vehicle is in a steering maneuver as shown in Figure 1 (b). This sideslip is measured by slip angle β:

$$\beta = \tan^{-1}\left(\frac{v_y}{v_x}\right) \tag{3}$$

where v_y is the lateral velocity due to the sideslip. As a result of the sideslip, the lateral force F_y is generated on the wheel in the opposite direction of v_y. The drawbar pull and lateral force are dependent on both the longitudinal and lateral slips, and in this paper, these relationships are also evaluated as grouser performances.

The relation among the slip ratio, slip angle, drawbar pull, and lateral force is also related to the traversability of inclined terrain for the wheel. Here assume that a wheel is ascending a slope of maximum inclination angle θ with an attack angle α as shown in Figure 2. Further assuming that the all the forces acting on the wheel are in equilibrium and the wheel is in steady state, then the following equations hold:

$$\frac{F_x}{W} = \sin\theta_p = \cos\alpha \sin\theta \tag{4}$$

$$\frac{F_y}{W} = \sin\theta_r = \sin\alpha \sin\theta \tag{5}$$

where W is the weight on the wheel whereas θ_p and θ_r are the pitch and roll angles of the wheel, respectively. That is, the higher drawbar pull and lateral force the wheel can produce, the steeper the slopes the wheel can traverse with lower slip.

3 Guideline for Grouser Spacing to Improve Drawbar Pull

3.1 Experimental apparatus and technique

Figure 3 shows the experimental apparatus used in this research, as well as in prior work [6] described briefly in this section. The single wheel test rig consists of a

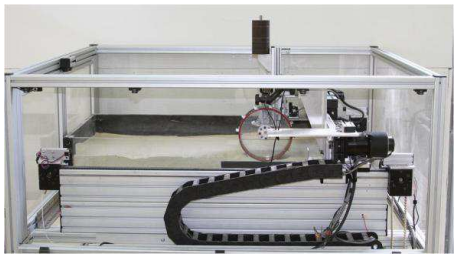

Figure 3. Single wheel test rig.

glass-walled soil bin, a wheel with a driving motor, an actuated longitudinal axis carriage, and an imaging system. The soil bin is filled with material of interest with 1.2 m length by 0.7 m width by 0.23 m depth. The longitudinal motion of the wheel is controlled by the carriage velocity in conjunction with the wheel angular velocity for a constant slip ratio during a test. The wheel can move freely in the vertical direction allowing natural wheel sinkage. The sinkage is measured by an optical encoder attached to the vertical free axis, and the forces on the wheel are measured by a six-axis force/torque sensor.

The glass wall of the soil bin and the imaging system can be used to observe and analyze soil flow as it interacts with a wheel. The soil optical flow technique (SOFT) is discussed in detail in [8]. Here it suffices to discuss results from SOFT experiments for grousered wheels.

Figure 4 shows observed soil flow for wheels with 16 grousers and with 48 grousers. The diameter and width of these wheels are the same, and the height of the grouser is also consistent for the two wheels. The magnitudes of the soil flow are plotted in the top images, with warmer colors indicating higher magnitude. Flow directions are shown in the bottom images, with the colors corresponding to directions shown in the color wheel in the bottom right corners.

The soil flow direction plots show periodic forward soil flow (yellow region) in front of the wheels with 16 grousers. The forward flow is induced after the rim of the wheel touches the soil surface and disappears after a grouser enters into the soil. With 48 grousers, however, no forward soil flow can be observed. This is because the grousers continuously excavate the soil before the rim touches the soil surface.

3.2 Grouser spacing equation

Based on the soil flow observations discussed above, an increase in the number of grousers can reduce the forward soil flow in front of the wheel. Forward soil flow causes an increase of motion resistance on the wheel, and thus decreases net drawbar pull. Therefore, by reducing resistive forward soil flow with a sufficient number of grousers it is possible to increase drawbar pull.

From this observation, a guideline for designing grouser spacing was derived. The basic idea is that the forward flow can be reduced if a grouser interacts with the

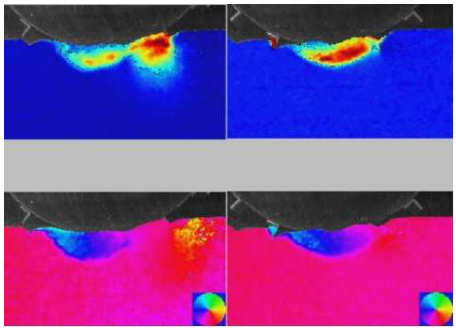

(a) Soil flows with 16 grousers

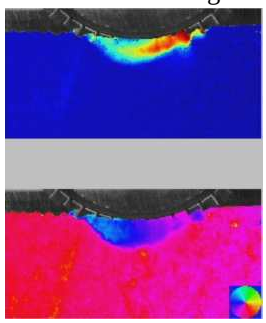

(b) Soil flow with 48 grousers

Figure 4. Top: magnitude of soil flow as wheels drive from left to right, bottom: direction of soil motion (shown according to colorwheel). With an insufficient number of grousers, a wheel experiences periodic resistive forward soil flow (yellow region in direction plot for wheel with 16 grousers) [6].

soil before the wheel rim advances into the ground ahead. The condition for this is geometrically obtained as [6]

$$\phi < \frac{1}{1-s}\left(\sqrt{\left(1+\hat{h}\right)^2-(1-\hat{z})^2}-\sqrt{1-(1-\hat{z})^2}\right) \quad (6)$$

where ϕ is the angle between two successive grousers, s is the wheel slip, $\hat{h}$ is the height of the grouser, and $\hat{z}$ is the wheel sinkage. Note that $\hat{h}$ and $\hat{z}$ are normalized by the wheel radius. Therefore required minimum number of grousers, $n_{\min}$, is given as

$$n_{\min} = \frac{2\pi}{\phi_{\max}} \quad (7)$$

where $\phi_{\max}$ is the maximum grouser spacing which satisfies the condition (6).

Some general predictions of this equation are that the minimum number of grousers required decreases with increasing slip and with increasing grouser height.

3.3 Experimental validation

To validate equation (7), experiments were conducted by using the test rig described in Section 3.1 with different grouser spacings. Two types of soil materials were

used: GRC-1 lunar soil simulant and Fillite. GRC-1 is a lunar regolith simulant developed by NASA Glenn Research Center [9]. Fillite is a commercial fly ash that is extremely weak and induces high sinkage. The mechanical properties of GRC-1 and Fillite are listed in Table 1. For each test, the soil was evenly loosened and leveled. Wheel with radius of 114 mm and width of 57 mm was used and pressed against the glass of the soil bin. Grousers of heights 6.3, 9.5, 12.7, or 25.4 mm were used while the number of grousers was varied to 0, 3, 6, 12, 16, 24, 32 or 48 for each height. The mass of the wheel was set to 10 kg and 5 kg for GRC-1 and Fillite, respectively.

Slip ratio of $s = 0.2$ was chosen for the test condition. This is because a wheel can generally achieve high tractive efficiency at slip ratio of around 0.1–0.3. Guidelines for selecting slip ratio to design grouser spacing is also discussed in [6]. The tests were conducted at least three times for each condition.

The obtained relations between the number of grousers and drawbar pull are shown in Figure 5. The averages of drawbar pull normalized by wheel weight are used in the plot. The required minimum numbers of grousers were computed from (7), using $s = 0.2$ and the sinkage of grousereless wheels, and listed in Table 2. These numbers are also shown in Figure 5 as dashed lines. As seen in Figure 5, the drawbar pull increases with the increase of the number of grousers in all the conditions; however, the rise in drawbar pull reaches a plateau when the wheel has a certain number of grousers. Eq. (7) successfully estimates the sufficient number of grousers over which the drawbar pull does not get much further increase even if the number of grousers increases.

The results suggest the grouser spacing equation (7) is valid for different soil materials and different heights of grousers. However, the equation is based on an analysis of straight grousers in simple forward travel. The next section discusses grouser spacing on wheels undergoing sideslip.

4 Influence of Grouser Spacing on Steering Performance

Previous related research has shown that increasing the number and height of grousers can improve the straight travel performance of wheels. In this study, tests

Table 1. Soil properties of GRC-1 and Fillite.

	GRC-1 [9]	Fillite [8]
Particle size [mm]	0.05–2	0.005–0.5
Bulk density [kg/m^3]	1600–1900	350–450
Friction angle [deg]	29.8–44.4	25–30
Cohesion [kPa]	< 1	~ 0

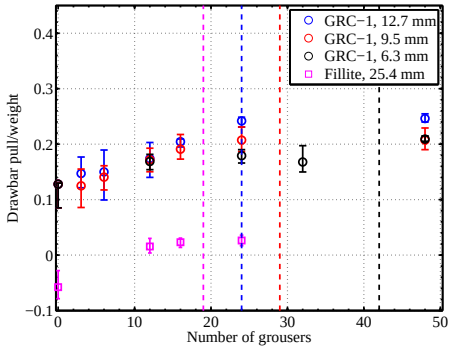

Figure 5. Drawbar pull vs. number of grousers for GRC-1 and Fillite. Drawbar pull plateaus with a sufficient number of grousers. The dashed lines show the predicted minimum number of grousers required to obtain high drawbar pull for each test condition.

Table 2. Computed minimum number of grousers.

Soil type	GRC-1			Fillite
Grouser height [mm]	6.3	9.5	12.7	25.4
Min. # of grousers	42	29	24	19

with different spacing (number) of grousers were carried out in sideslip operations, to assess the influence of spacing on steering performance of a wheel.

4.1 Experimental method and condition

In the experiment, GRC-1 soil was used. A wheel with radius of 114 mm and width of 114 mm was utilized. For assessing the influence of grouser spacing, 0, 12, or 24 grousers of 12.7 mm height were set on the wheel. The mass of the wheel was fixed to 10 kg for each condition.

The orientation, or slip angle, of the wheel was changed from 0 to 30 deg with an interval of 7.5 deg to make artificial sideslip motion as shown in Figure 6. For each slip angle condition, the wheel slip ratio was set to 0, 0.2, 0.4, or 0.6. During the tests, the wheel was controlled to rotate with constant tangential velocity of 10 mm/s while the speed of the carriage was controlled depending on the desired slip ratios and slip angles. Tests were conducted in duplicate for each test condition.

(a) $\beta = 15$ deg (b) $\beta = 30$ deg

Figure 6. Test wheel with sideslip configurations.

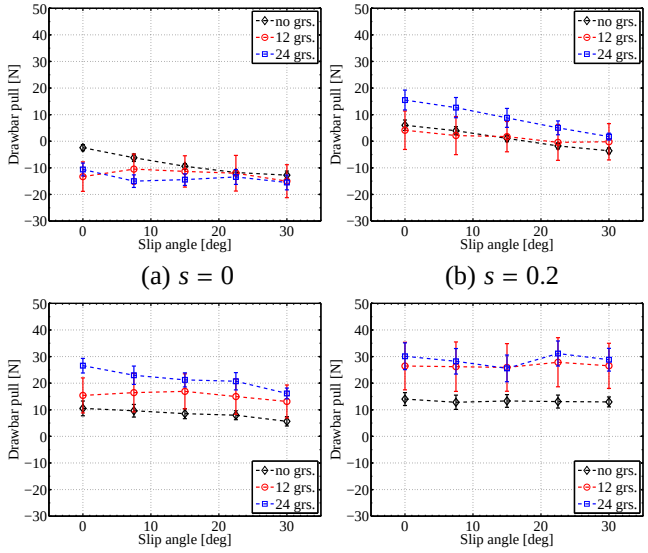

(a) s = 0 (b) s = 0.2

(c) s = 0.4 (d) s = 0.6

Figure 7. Influence of grouser spacing on drawbar pull during sideslip.

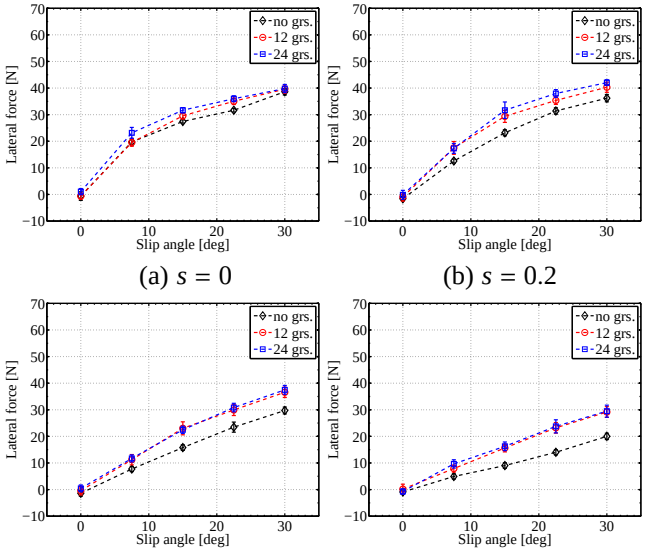

(a) s = 0 (b) s = 0.2

(c) s = 0.4 (d) s = 0.6

Figure 8. Influence of straight grousers on lateral force during sideslip.

4.2 Experimental result

The results of sideslip tests with different number of grousers are shown in Figure 7 and Figure 8. The markers show the average values of drawbar pull and lateral force with the standard deviations as error bars.

The grouser spacing equation (7) predicts that the minimum required number of grousers decreases with increasing slip. The results in Figure 7 indicate that this prediction remains valid in sideslip operations. During sideslip tests, 24 grousers are shown to produce significantly higher drawbar pull than 12 grousers at 20 percent slip, but produce little to no discernable advantage over 12 grousers at 60 percent slip. Thus at 60 percent slip, drawbar pull has already reached a plateau with 12 grousers, while as 20 percent slip operation it has not, and additional grousers are required to gain higher drawbar pull.

In Figure 7 we also see that drawbar pull decreases with increasing sideslip angle at low slip, but that it is not sensitive to sideslip angle at higher slip.

Figure 8 shows the lateral force increases along with the increase of the slip angle and decreases with the increase of the slip ratio. The figure also shows that grousers generally increase lateral force in all sideslip conditions, but the differences between 12 and 24 grousers are smaller compared to the drawbar pull.

5 Influence of Grouser Chevron Angles on Traversing Performance

Experiments with different angles of chevron grousers were conducted to evaluate chevron grousers on both straight travel and steering performance of wheels.

(a) Orientation (b) θ_g= 30 deg (c) θ_g = -30 deg

Figure 9. Orientations of chevron grousers.

5.1 Experimental method and condition

In the experiment, GRC-1 soil was used, and a wheel with radius of 114 mm, width of 114 mm, and mass of 10 kg was utilized as in the experiments in Section 4. For assessing the influence of chevron angles of grousers, different angles of chevron-shaped grousers were mounted on the wheel rim. Positive chevron angle θ_g is defined in the direction in which grousers engage the soil along the wheel rotation whereas negative ones are in the direction where grousers sweep the soil away to the side as shown in Figure 9. The orientation of the grousers was varied from -45 to 45 deg with an interval of 15 deg. In each pattern, the number and height of the grousers were consistent as 24 and 12.7 mm, respectively.

5.1.1 Straight travel test

In the straight travel test, the wheel was controlled to rotate with constant tangential velocity of 10 mm/s, and the carriage speed was controlled to make an constant wheel slip ratios. The slip ratio was varied from 0.1 to 0.9 with an interval of 0.1. Tests were conducted three times for each test condition.

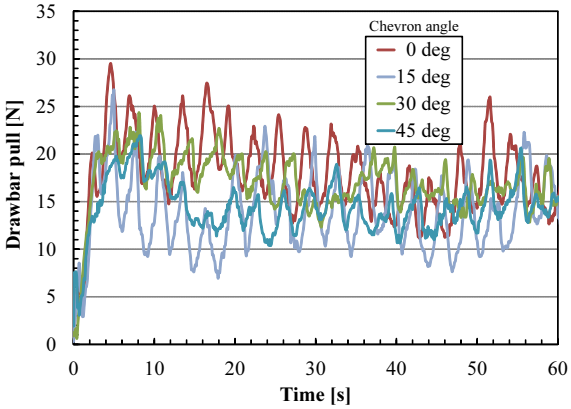

Figure 10. Time variances of drawbar pull at $s = 0.2$. Steeper chevron angles reduce variability (amplitude).

5.1.2 Sideslip test

In this test, the slip angle of the wheel was changed from 0 to 30 deg with an interval of 7.5 deg. For each slip angle condition, the wheel slip ratio was set to 0, 0.2, 0.4, or 0.6. Each test was conducted twice.

5.2 Experimental results

5.2.1 Results of straight traveling test

Figure 10 shows time variances of the drawbar pull with different chevron angles at the slip of $s = 0.2$. The drawbar pulls vary periodically according to the grouser-soil interactions. As seen in the figure, the variance in drawbar pull is largest with straight grousers and decreases with the increase of the chevron angle of grousers. This is because steeper grousers can more continuously contact with the soil while the interaction of straight grousers is more discrete.

The relation between wheel slip ratio and the drawbar pull, sinkage, and tractive efficiency are shown in Figure 11. In Figure 11 (a), we can see that the drawbar pull decreases with the increase of the grouser chevron angles, especially at high slip rate. For example, at the slip ratio of $s = 0.8$, the drawbar pull of straight grousers is 12.3%, 9.9%, and 23.2% higher than that of 15, 30, and 45 deg chevron grousers, respectively. That is, according to Eq. (4), the wheel with straight grousers can ascent 3.0, 2.5, and 5.7 deg steeper slopes than the wheels with 15, 30, and 45 deg chevron grousers, respectively, at the slip condition. When compared to the positive and negative orientations, negatively oriented grousers tend to gain higher drawbar pull.

The sinkage does not drastically change among different grouser orientations as shown in Figure 11 (b). However, grousers with steeper orientation induce higher sinkage, and positive orientations result more sinkage than negative ones, especially at high slip conditions. This may

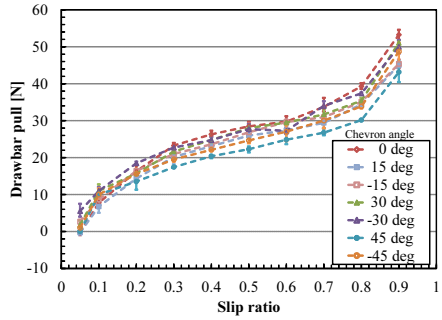

(a) Slip vs. drawbar pull

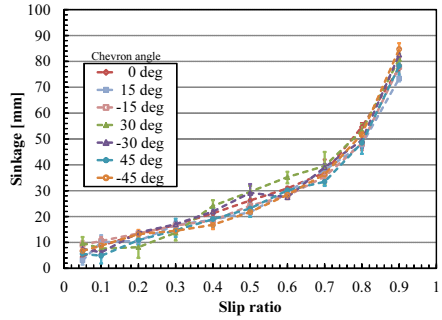

(b) Slip vs. sinkage

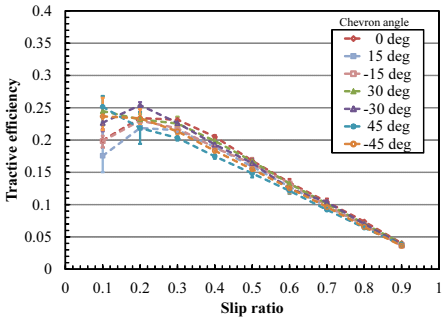

(c) Slip vs. tractive efficiency

Figure 11. Straight traveling performance for different grouser orientations. Chevron grousers appear to improve drawbar pull and tractive efficiency at low slip.

be because positively oriented chevron grousers transport larger amounts of soil from the front to rear of the wheel causing higher sinkage. This higher sinkage makes higher motion resistance for chevron grousers, thus lower drawbar pull as shown in Figure 11 (a).

Steeper chevron grousers gain higher tractive efficiency at low slip conditions ($s < 0.2$) as shown in Figure 11 (c). Because continuous soil contacts of chevron grousers requires less wheel torque than straight grousers, the efficiencies of steeper grousers become higher at low slip conditions. On the other hand, at higher slip, however, straight grousers gain higher tractive efficiency than chevron grousers because of their high drawbar pull compared to chevron grousers.

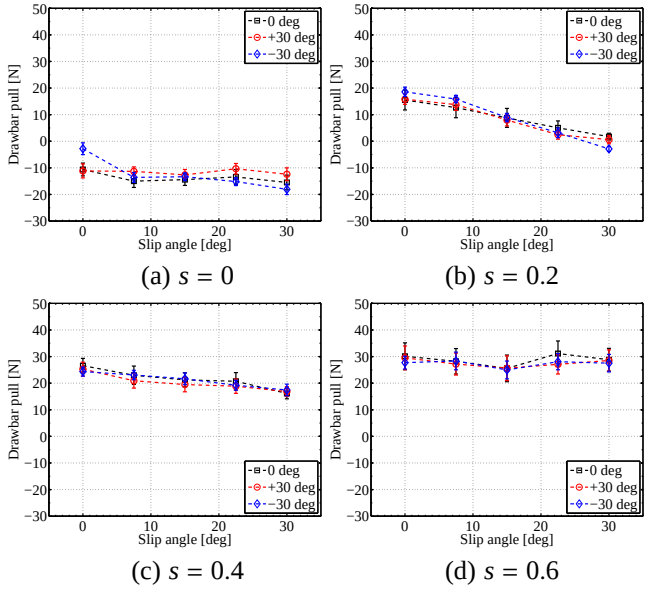

(a) $s = 0$ (b) $s = 0.2$

(c) $s = 0.4$ (d) $s = 0.6$

Figure 12. Influence of grouser orientation on drawbar pull during sideslip.

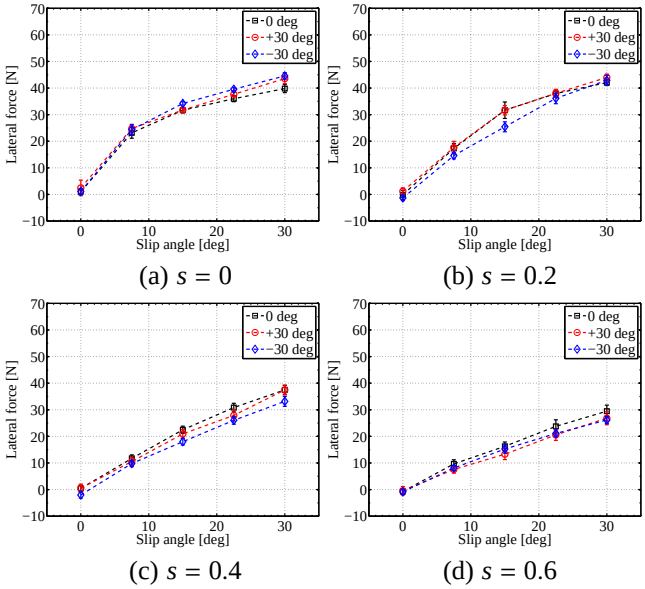

(a) $s = 0$ (b) $s = 0.2$

(c) $s = 0.4$ (d) $s = 0.6$

Figure 13. Influence of grouser orientation on lateral force during sideslip.

5.2.2 Results of sideslip test

The relationships between the slip angle and drawbar pull and lateral force are shown in Figure 12 and 13, respectively, for the grouser orientation of 0, 30, and -30 deg. As seen from Figure 12, the trends of drawbar pull against the slip angle are similar for all the orientations. That is, the drawbar pull decreases with increasing slip angle at low slip conditions, but at the high slip condition, the drawbar pull does not change largely. The differences of drawbar pull are not large for different grouser orientations compared to the influence of slip ratio and slip angle.

The lateral force also shows the similar tendencies for all the chevron angles as shown in Figure 13. Again, the force increases with the increase of the slip angle and decreases with the increase of the slip ratio. The orientation of grousers has more influence on the lateral force than the drawbar pull. At the slip ratio of $s = 0$, the chevron grousers gain higher lateral force than straight grousers, especially at large slip angles. However, when the slip ratio increases, the lateral force of straight grousers becomes larger than that of chevron grousers.

6 Discussion on Grouser Designs

In this section, we will discuss grouser design guidelines for traversing loose, granular soils depending on vehicles' steering mechanism and types of terrain for operations.

6.1 Steering mechanism

Skid steering Skid steering utilizes sideslip of wheels. However, grousers can hamper skid steering due to increased lateral forces, as shown in previous sections. This must be traded off against increases in drawbar pull if considering a skid steer planetary rover with grousers. An interesting direction for future work could be investigating whether a greater number of smaller height grousers might mitigate increased lateral forces while maintaining advantageous drawbar pull.

Explicit steering If a rover has actuators for steering, grousers can improve the efficiency of the steering increasing the wheel drawbar pull and decreasing the lateral force. Therefore, grousers should be designed depending on the target terrain as discussed next. Future work could test resistance forces associated with turning a wheel in place. It is expected that the net steering resistance from such maneuvers should be lower than skid steering, which would make explicit steering a good choice for wheels with grousers.

6.2 Terrain type

Benign terrain If a vehicle is supposed to mainly operate on benign terrain or gentle slopes, the vehicle does not require high drawbar pull. In this case, grousers with an orientation can be recommended such as, chevron or zigzag shapes, since these grousers can continuously contact with the soil enabling the vehicle travels smoothly and achieves higher tractive efficiency than straight grousers at low slip.

Steep slopes or highly weak soil If the mission's primal target area of interests are inclined slopes, such as sand dunes, flank of mountains, or crater rims, the wheels will

likely experience high slip in both longitudinal and lateral directions. Also, if the terrain is composed of highly weak materials, significant slip and sinkage can occur even if the terrain is level. In such conditions, straight grousers can help obtain large drawbar pull and lateral force to overcome the difficult terrain.

7 Conclusions

This work extends grouser studies to include chevron-shaped grousers and also sideslipping motions for cross-slope and steering maneuvers.

Prior work by the authors developed an equation for appropriate grouser spacing, based on the elimination of periodic resistive forward soil flow, that had been observed sub-surface experimentally. In this work, minimum numbers of grousers, predicted by this equation, are shown to also be consistent with new experiments in a different type of granular soil, suggesting robustness of the equation to soil type. Some general predictions of this equation are that the minimum number of grousers required decreases with increasing slip and with increasing grouser height. This work shows that the prediction of a lower minimum number of grousers at higher slip remains valid in sideslip operations.

This work shows that chevron-shaped grousers can increase tractive efficiency (the ratio of output to input work for a wheel) at low slip. This is attributed to reduced variation in drawbar pull with chevron angle, which may likely be caused by the more gradual and overlapping engagement of chevron grousers with soil. The dependency on low slip makes chevrons particularly suitable for flat benign terrains where efficiency is of paramount importance. For steep slopes or other challenging terrains, straight grousers may still be preferable in the tradeoff of peak performance for average efficiency.

This research also shows that grousers increase lateral forces during sideslip operations, regardless of the grouser orientation. This characteristic of grousers can be particularly useful for improving performance in terrains where a rover is required to traverse cross-slopes. However, it also points out a drawback of combining grousers with skid-steering, as lateral forces decrease skid-steering efficiency.

Acknowledgment

This work has been supported by grants from the Jet Propulsion Laboratory (SURP 1492245) and NASA Glenn Research Center (NNX13AD45A). The authors would like to thank Matt Heverly and Scott Moreland of the JPL and Colin Creager of GRC for their support, advice and analysis of the methods and results of the experimentation described in this paper.

References

[1] M. Bauer, W. Leung, and T. Barfoot, Experimental and simulation results of wheel-soil interaction for planetary rovers, In *proceedings of the 2005 IEEE/RSJ International Conference on Intelligent Robots and Systems*, Edmonton, August, 2005.

[2] M. Sutoh, J. Yusa, T. Ito, K. Nagatani, and K. Yoshida, Traveling performance evaluation of planetary rovers on loose soil, *Journal of Field Robotics*, vol.29 (4), 2012, pp.648–662.

[3] L. Ding, H. Gao, Z. Deng, K. Nagatani, and K. Yoshida, Experimental study and analysis on driving wheel¢¢s performance for planetary exploration rovers moving in deformable soil, *Journal of Terramechanics*, vol.48, (1), 2011, pp.27–45.

[4] R. Irani, R. Bauer, and A. Warkentin, A dynamic terramechanic model for small lightweight vehicles with rigid wheels and grousers operating in sandy soil, *Journal of Terramechanics*, vol.48 (4), 2011, pp. 307–318.

[5] H. Nakashima, H. Fujii, A. Oida, M. Momozu, H. Kanamori, S. Aoki, T. Yokoyama, H. Shimizu, J. Miyasaka, and K. Ohdoi, Discrete element method analysis of single wheel performance for a small lunar rover on sloped terrain, *Journal of Terramechanics*, vol.45 (5), 2010, pp. 307–321.

[6] K. Skonieczny, S. J. Moreland, and D. S. Wettergreen, A grouser spacing equation for determining appropriate geometry of planetary rover wheels, In *proceedings of the 2012 IEEE/RSJ International Conference on Intelligent Robots and Systems*, Vila Moura, October, 2012.

[7] J.Y. Wong, *Theory of Ground Vehicles*, the 4th edition, John Wiley & Sons, 2008.

[8] K. Skonieczny, S.J. Moreland, V.M. Asnani, C.M. Creager, H. Inotsume, and D.S. Wettergreen, Visualizing and analyzing machine-soil interactions using computer vision, *Journal of Field Robotics*, *in press*, DOI: 10.1002/rob.21510.

[9] H. Oravec, V. Asnani, and X. Zeng, Design and characterization of GRC-1: A soil for lunar terramechanics testing in Earth-ambient conditions, *Journal of Terramechancis*, vol.47, 2010, pp.361–377.